

## Removal of Crystal Violet by wet oxidation with H<sub>2</sub>O<sub>2</sub> over an Iron oxide catalyst synthesized from Fly Ash

Y. Benjelloun<sup>1,2\*</sup>, A. Lahrichi<sup>2</sup>, S. Boumchita<sup>1</sup>, M. Idrissi<sup>2</sup>, Y. Miyah<sup>1</sup>,  
Kh. Anis<sup>1</sup>, V. Nenov<sup>3</sup>, F. Zerrouq<sup>1</sup>

<sup>1</sup>QHSE Research Group, Laboratory of Catalysis, Materials and Environment, University of Sidi Mohammed Ben Abdellah, School of Technology, BP 2427 Fez - Morocco

<sup>2</sup>Laboratory biochemistry, Faculty of Medicine and of Pharmacy, University Sidi Mohammed Ben Abdellah – Morocco

<sup>3</sup>Burgas Asen Zlatarov University, Bulgaria.

Received ...

Keywords

- ✓ Fly Ash,
- ✓ Crystal Violet,
- ✓ Wet impregnation,
- ✓ Iron oxide,
- ✓ Catalytic oxidation,
- ✓ Hydrogen peroxide.

\*Corresponding Author  
[youssef.benjelloun1@usmba.ac.ma](mailto:youssef.benjelloun1@usmba.ac.ma)  
Phone: +212669643051

### Abstract

In order to recover and utilize waste coal generated by thermal power plants, Fly Ash (FA) was employed in this research to treat contaminated wastewater. Generally, a preliminary washing treatment of raw FA with ultra pure water was necessary. Rather FA provided a high surface area for the deposition of iron oxide from its precursor solution; it also acted as a support during wet impregnation process. The morphology and structure of raw FA, washed FA and synthesized Fe/FA Catalyst (Fe-FAC), were investigated by two analytical methods included, powder X-ray diffraction (XRD) and scanning electron microscopy (SEM). As one of the most persistent and largely applied synthetic dyes, Crystal Violet (CV) may pose a dangerous risk to the environment. Therefore, the catalytic activity of Fe-FAC was evaluated by the wet oxidation of CV using hydrogen peroxide (H<sub>2</sub>O<sub>2</sub>). The influence of some important parameters such as, catalyst dose, precursor load, initial dye concentration, H<sub>2</sub>O<sub>2</sub> amount, pH and temperature were studied as well. Significantly, the Fe-FAC/H<sub>2</sub>O<sub>2</sub> process enhanced the removal of CV under optimum conditions revealed according to this study.

### 1. Introduction

Wastewater released from textile, paper, cosmetic food, paint, leather, printing and photography industries contains some recalcitrant pollutants; especially synthetic dyes. A considerable amount of these dyes is present in industrial effluents due to losses in the process [1]. Most organic dyes create acute issues in the ecosystem as they are toxic, mutagenic and carcinogenic for aquatic life and humans [2, 3]. Therefore, more efficient and economical technologies are needed for the treatment of contaminated wastewater. Consequently, there are many researchers trying to explore processes that are more reliable and eco-friendly for the removal of dyes from industrial effluents including biological, physical and chemical processes [4, 5]. Using some of these methods is limited for different reasons; for example, the adsorption can represent a viable solution [6], but it has the disadvantage of transferring the pollutant onto the adsorbent. As well, the chemical coagulation and ion exchange processes [7] could remove dyes reasonably, but it would produce a large amount of sludge, which causes another waste problem. Also for the activated carbon processes that can remove dyes in aqueous solution effectively, but the material and the subsequent treatment are very costly [8].

In the last decade, attention has focused on Advanced Oxidation Processes (AOPs), based on the generation of highly reactive hydroxyl radicals. When the nature of the pollutant is clearly identified, catalytic oxidation can be used to significantly increase the oxidation rate of the target molecule. Depending on the oxidant used,

several processes can be envisaged: Catalytic Wet Air Oxidation (CWAO) [9], Catalytic Wet Ozonation (CWO) with O<sub>3</sub> [10], and Catalytic Wet Peroxide Oxidation (CWPO) with H<sub>2</sub>O<sub>2</sub> [11, 12].

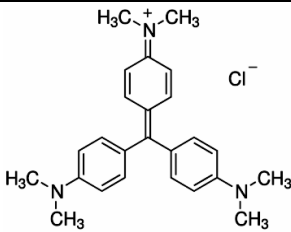
Several researchers have proposed different strategies, including composites based on organic/inorganic materials which are used as supports for catalysts synthesis [13, 14]. Fly Ash (FA) may provide a suitable surface for incorporation of these materials, preventing their agglomeration. FA is a coal combustion by-product generated in very large quantities from coal thermal power plants around the globe and consists of fine, powdery particles with a spherical shape [15]. In the recent few years, many studies have investigated effective ways to modify FA for valuable applications; such as their utilization as an additive in the manufacturing of cement, concrete, construction materials, road pavement and use of fly ash in zeolite synthesis for wastewater treatment [16, 17].

This paper reports on synthesis, characterization and evaluation of catalytic performance of synthesized FA catalysts. The chemical oxidation, by CWPO process, of Crystal Violet (CV) in aqueous solution was selected as the test reaction model, knowing that CV is the typical synthetic dye as it is a mutagen - mitotic poison and toxic to mammalian cells [18]. The factors which affect the catalytic activity, such as catalyst dose, precursor load, initial dye concentration, hydrogen peroxide amount, pH solution and temperature were investigated.

## 2. Experimental

### 2.1. Materials

FA used in this study are generated in the thermal power Jorf Lasfar Energy Company (JLEC) following the burning of coal from South Africa. The FA contains element oxides such as SiO<sub>2</sub> (52.07%), Al<sub>2</sub>O<sub>3</sub> (23.34%), Fe<sub>2</sub>O<sub>3</sub> (8.86%), CaO (1.95%), MgO (1.09%), SO<sub>3</sub> (1.87 %), K<sub>2</sub>O (1.9%), Na<sub>2</sub>O (0.4 %) and Loss on Ignition (8.52%) [19]. In the present work we tried to utilize the coal fly ash as a support for catalysts preparation. A preliminary washing treatment of raw fly ash with ultra pure water represents a basic step for successful processing of such a material [20]. Iron (III) Chloride Hexahydrate (FeCl<sub>3</sub>.6H<sub>2</sub>O) was used as the precursor. Hydrogen Peroxide 30% (w/V) was used as the oxidant. Both reagents were purchased from “Biotechnics Solution Company”. In this study, Crystal Violet dye (CV) in the Table 1, was selected as a model pollutant due to its toxicity, poisoning, ease of analysis, and relative solubility in water [21]. CV dye was provided by “Sigma–Aldrich Company” and directly dissolved from pure CV.

<b>Structural Formula</b>	
Chemical Name	Crystal Violet
Molecular Formula	C <sub>25</sub> H <sub>30</sub> ClN <sub>3</sub>
Molecular Weight	407.98 g/mol
Maximum wavelength λ max	588 nm

**Table 1:** Structure and characteristics of Crystal Violet dye.

### 2.2. Methods

#### 2.2.1. Synthesis of the Fly Ash catalyst

The raw FA were washed with ultra-pure water under magnetic stirring at room temperature for 24h, in order to remove the soluble compounds K<sub>2</sub>O, Na<sub>2</sub>O, MgO, CaO. The ratio between raw FA and ultra-pure water was 1:10 [g/ml]. Then the suspension was filtered and dried at 105-115 °C for 24 h. Further, the sample was dried and cooled, it was grounded, homogenized and finally sieved; the fraction 125µm was selected.

Briefly, the catalyst powder was synthesized by the wet impregnation method, using washed FA as a support, according to the following procedure: Firstly, the required quantity of washed FA was contacted with an aqueous solution of Iron III Chloride ( $\text{FeCl}_3$ ) in order to obtain catalysts with Fe metal load of 1, 3 and 5 wt%. Secondly, the solution was left under continues stirring then the slurry was heated at 90 °C to vaporize the aqueous water. Thirdly, the sample was dried at 105 °C in an oven for overnight. Finally, the mixtures were ground and calcined in air at 500 °C for 4 h, to obtain the Fe-FA catalysts (Fe-FACs). This process allows obtaining catalysts with high mechanical strength and good dispersion of the active phase [22].

### 2.2.2. Characterization

- *XRD analysis*

The identification of the samples crystalline structure was performed using powder X- ray diffraction (XRD) (Diffractometer X'Pert PRO / X'Celerator) of Panalytical Company. The operating conditions were 40kV and 30 mA, using Cu  $K\alpha$  ( $\lambda = 1, 54060$  nm) radioactive source and over the  $2\theta$  range 10°- 80°.

- *SEM analysis*

As reported in literature [23], scanning electron microscopy (SEM) is one of the best and most widely used techniques for the chemical and physical characterization of FAs. In this work, the surface morphology of the synthesized catalysts and the FA particles were examined with a SEM (Quanta 200 FEI) instrument.

### 2.2.3. Experimental procedure for catalytic degradation of CV

The degradation process was established by observing the catalytic activity of the Fe-FAC for oxidation of CV using  $\text{H}_2\text{O}_2$  as the oxidizing reagent, at room temperature using the batch processing technique [24]. Initially, all experiments were carried out in a 250 ml glass beaker, containing 100 ml of CV dye aqueous solution. Predetermined amounts of Fe-FAC were then added to the beaker and the mixture was allowed to reach equilibrium then  $\text{H}_2\text{O}_2$  was added also, this was recorded as the starting time of the reaction. Moreover, 4 ml of each sample was extracted at 5 min intervals for 150 min, the extracted solution was filtered using a syringe filter of diameter 0,45 $\mu\text{m}$  (Minisart, sartorium stedim biotech) to separate catalyst particles from the solution. The measurement was evaluated immediately at  $\lambda$  max= 588nm by UV - visible spectrophotometer 1240 SHIMADZU. Each sample was suspended by stirring during measurement. The absorbance level was analyzed by the corresponding wavelength from the UV-vis spectrophotometer.

The removal rate of CV was calculated by the following equation [25]: Where  $C_0$  is the initial dye concentration and  $C_t$  is dye concentration after t: time (min).

$$\% \text{ Removal} = \left( \frac{1 - C_t}{C_0} \right) \times 100 \quad (1)$$

Furthermore, for the evaluation of the removal rate, the experimental data are fitted by applying a pseudo- first order kinetics model defined by Mathews & Weber equation [26], with  $K$  ( $\text{min}^{-1}$ ) is the reaction rate constant:

$$\ln \left( \frac{C_t}{C_0} \right) = -Kt \quad (2)$$

Various factors such as, catalyst dose (0.25 - 1.25 g/l), precursor load (1 - 5%), initial dye concentration (20 - 50 ppm),  $\text{H}_2\text{O}_2$  amount (0.19 - 1.96 M), pH solution (5 - 11) and  $T^\circ$  (20° - 50°C) were studied.

## 3. Results and discussion

### 3.1. Characterization of FA particles and Fe-FAC

#### 3.1.1. XRD analysis-Semi-quantitative analysis

XRD / Semi-quantitative data processing allow comparing spectral data in order to obtain information regarding the relative concentrations of elements.

	<i>Mineral phase</i>	<i>Chemical Formula</i>	<i>Semi Quantitative (%)</i>
<i>Washed FA</i>	Mullite	Al <sub>4.75</sub> Si <sub>1.25</sub> O <sub>9.63</sub>	76
	Quartz	Si O <sub>2</sub>	24
<i>Fe-FA Catalyst</i>	Mullite	Al <sub>4.75</sub> Si <sub>1.25</sub> O <sub>9.63</sub>	68
	Quartz	Si O <sub>2</sub>	14
	Hematite	Fe <sub>2</sub> O <sub>3</sub>	18

**Table 2:** Summary of the XRD / Semi-quantitative analysis.

It is observable in the semi-quantitative analysis (Table 2), the presence of Mullite and Quartz in washed FA with the relative concentrations of 76% and 24% successively. In contrast to Fe-FAC a lower percentage the two mineral phases (68% and 14%) was ascertained with a distinctly relative rate of iron oxide towards 18%.

XRD analysis was performed to investigate the crystal structure of mineral phases. The qualitative XRD results of washed FA are given in Fig. 1a ; whereas the XRD patterns of Fe-FAC were illustrated in Fig. 1b.

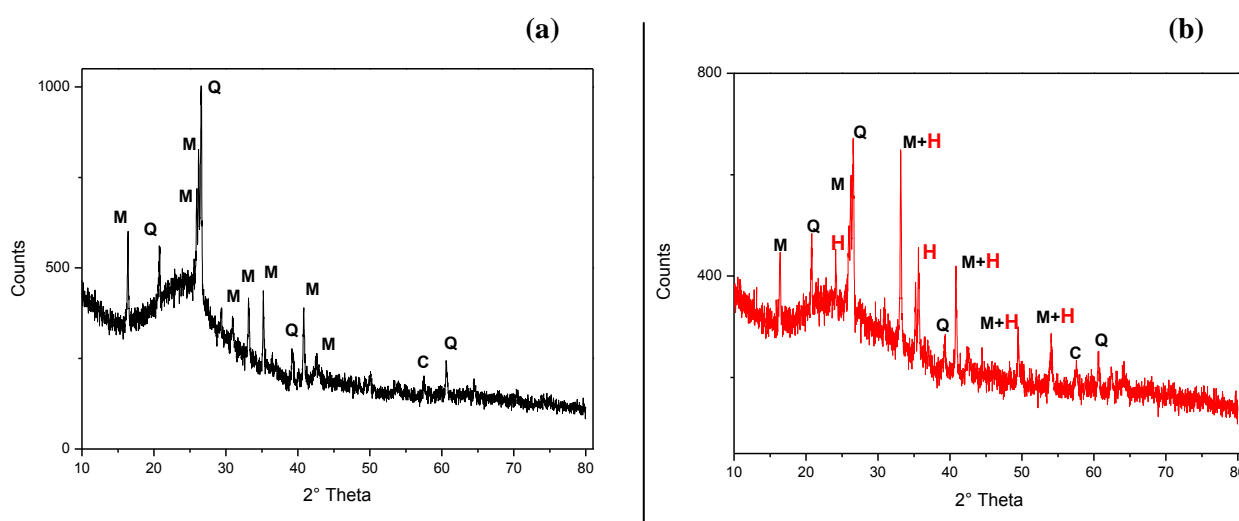


**Figure 1:** X- Ray Diffraction patterns of (a): washed FA and (b): Fe-FAC, (Q = Quartz, M = Mullite, C = Calcite, H = Hematite).

The major crystalline components of washed FA as shown in Fig. 1a were: Quartz (SiO<sub>2</sub>) identified by the sharp peak at  $2\theta = 26.54^\circ$ , along with the peaks related to Mullite (3 Al<sub>2</sub>O<sub>3</sub>. 2 SiO<sub>5</sub>) and the minor Calcite (CaCO<sub>3</sub>) peak at  $2\theta = 57.53^\circ$  with the coexistence of an amorphous phase. What is more, the intensity of quartz is very strong with Mullite, provided a suitable surface for the deposition. The low calcium oxide intensity is characteristic of low-Ca Class-F fly ash and similar to that reported in the literature [27].

The XRD pattern of Fe-FAC (Fig. 1b) showed additional peaks at  $2\theta = 24.14^\circ$ ,  $35.6^\circ$  corresponding to Hematite (Fe<sub>2</sub>O<sub>3</sub>) above all the peaks of washed FA, In addition, it can be observed four overlying peaks of Mullite and Hematite at  $2\theta = 40.81^\circ$ ,  $33.13^\circ$ ,  $49.44^\circ$  and  $54.08^\circ$ . As a result, also, the intensity decreased compared to the peaks of washed FA indicating the incorporation of iron oxide on the surface.

### 3.1.2. SEM analysis

Representative SEM images of raw FA, washed FA and Fe-FAC are illustrated in Fig. 2, which shows size, shape and dispersal of the samples components. The morphology of a fly ash particle is controlled by combustion temperature and cooling rate. The SEM data clearly indicated intermixing of iron (Fe) and aluminosilicates (Al-Si) mineral phases and the relative amount of aluminum and silicon varied from sphere to sphere and the size distribution also varied.

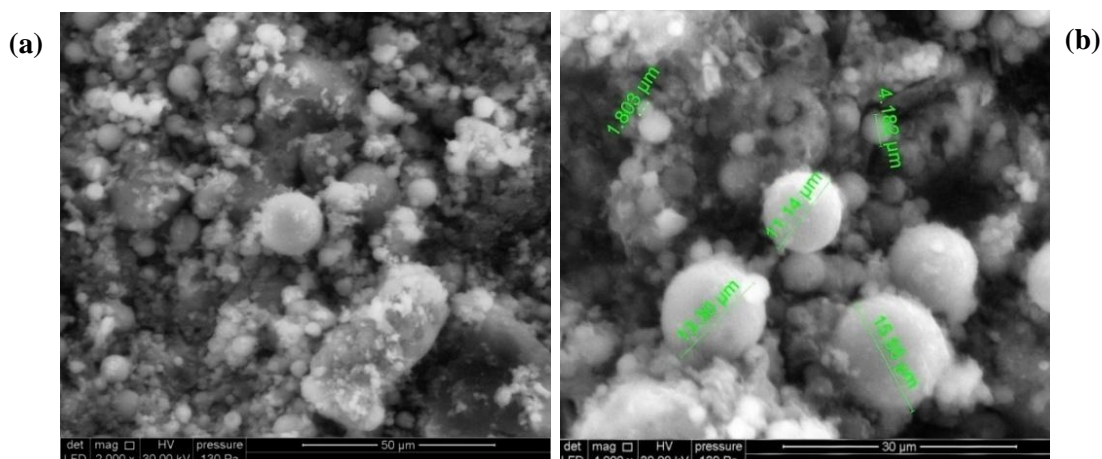


**Figure 2:** SEM Images of (a): raw FA, (b): washed FA.

The surface characteristics of raw FA were much different from washed FA; not only irregularly unburned carbon and non-shaped amorphous particles over the whole matrix in Fig. 2a; but also, washed FA particles possessed well shaped and well dispersed spheres over the surface. In the same way, the majority of the particles are ranged in size from approximately 1 $\mu$ m to 20  $\mu$ m and consisted of typical FA spheres (Fig. 2b).

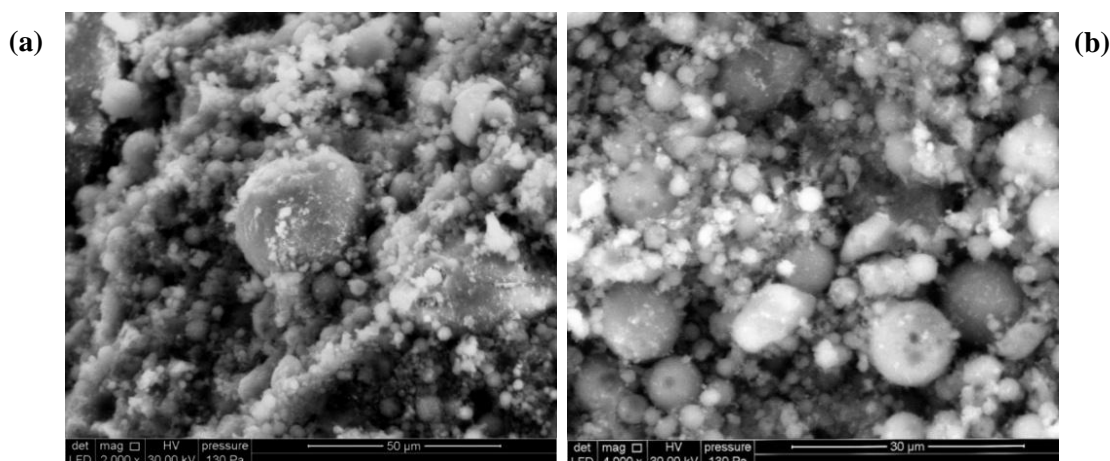


**Figure 3:** SEM Images of (a): washed FA, (b): Fe-FAC.

Many hydrates produced in the washing treatment formed large aggregated particles as exposed in Fig. 3a. The introduction of the precursor during the wet impregnation process influenced the surface topography of the material. The grains of the metals could be seen clearly in Fig. 3b, significantly distributed over the smooth surfaces of spherical Al-Si particles, which size's was admittedly decreased, so the surface area increased. Mainly, the bright areas indicated the existence of iron oxide. These results supported data obtained from previous leaching studies and were consistent with XRD data [23].

### 3.2. Treatment efficiency of Fe-FAC/ H<sub>2</sub>O<sub>2</sub> Process

#### 3.2.1. Kinetics of the catalytic degradation of CV

One of the primary aims of this investigation was to study the removal efficiency of CV by the Fe-FAC/H<sub>2</sub>O<sub>2</sub> process. Figure 4 shows the semi log plot of the CV concentration in terms of reaction time. A straight line plot showed that the degradation of CV is a pseudo first-order reaction. The rate constant  $k$  was calculated for Fe-FAC/ H<sub>2</sub>O<sub>2</sub>, from the slope of the line and the value obtained is  $k = 0.3688 \text{ min}^{-1}$ , with  $R^2 = 0.99443$ .



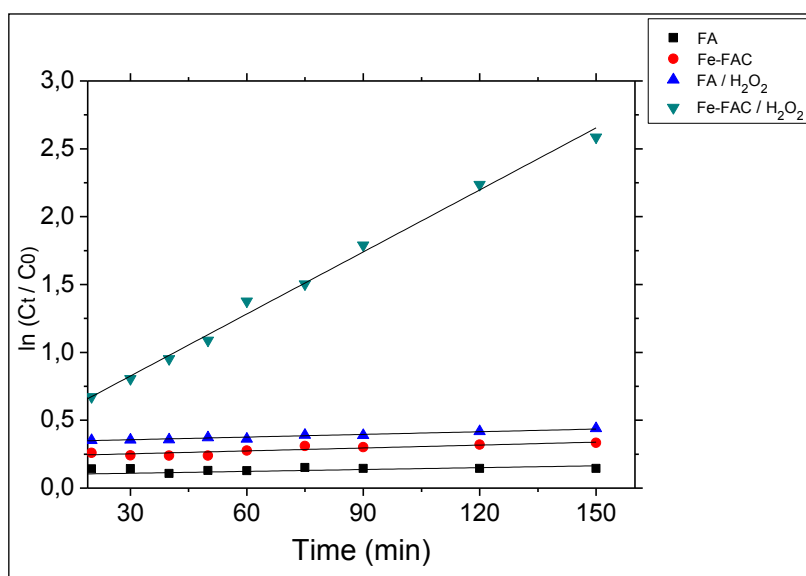


**Figure 4:** First-order kinetic plots for CV degradation in terms of time.

Exp. Conds: (Catalyst dose = 0.5g/L, Fe load = 3%, [CV]<sub>0</sub> = 20 ppm, [H<sub>2</sub>O<sub>2</sub>] = 0.39 M, natural pH, room T°).

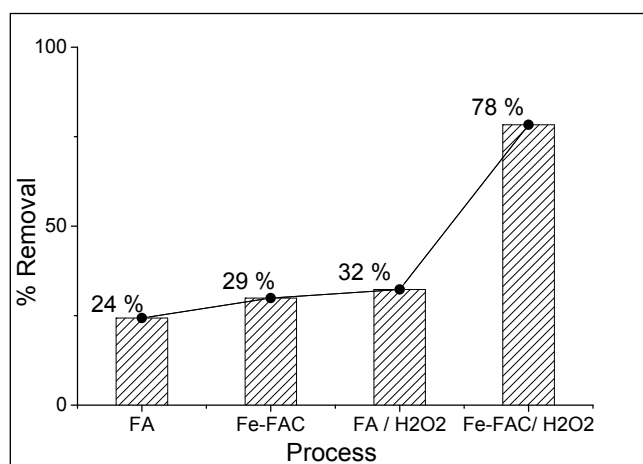


**Figure 5:** Comparative of CV removal efficiency in terms of various processes, at t= 90 min.

The removal efficiencies of the different processes studied (FA, Fe-FAC, FA / H<sub>2</sub>O<sub>2</sub>, Fe-FAC/ H<sub>2</sub>O<sub>2</sub>) were 24%, 29%, 32%, and 78%, respectively. As shown in Fig. 5, without H<sub>2</sub>O<sub>2</sub>, the removal efficiency of FA process was approximately the same as that of the Fe-FAC; less than 30% discoloration of CV were achieved, which was attributed to the adsorption capability of the used materials and chemical stability of CV. The presence of the oxidant in FA / H<sub>2</sub>O<sub>2</sub> process is not effective for the treatment of CV. This is probably due to very limited catalytic reactions between H<sub>2</sub>O<sub>2</sub> and an insubstantial amount of iron oxide. Instead, the removal efficiency of Fe-FAC / H<sub>2</sub>O<sub>2</sub> process (78%) was 49% higher than that of the Fe-FAC process. This result indicated that the combination of Fe-FAC and H<sub>2</sub>O<sub>2</sub> improved CV degradation rate.

### 3.2.2. Study of various experimental parameters affecting removal efficiency

Fe-FA/ H<sub>2</sub>O<sub>2</sub> process was evaluated by changing one parameter while the others were kept constant.

- *Effect of catalyst dose*

A number of reports [28] have demonstrated that catalyst dose has a large influence on the removal efficiency. Figure 6 displays the CV removal rate in terms of time for different catalyst doses (0.25 to 1.25 g/L), where the operating conditions were: 20 ppm of CV solution, 0.39 M of hydrogen peroxide over the 1% Fe-FAC catalyst, reactions were run with pH solution and at room Temperature.

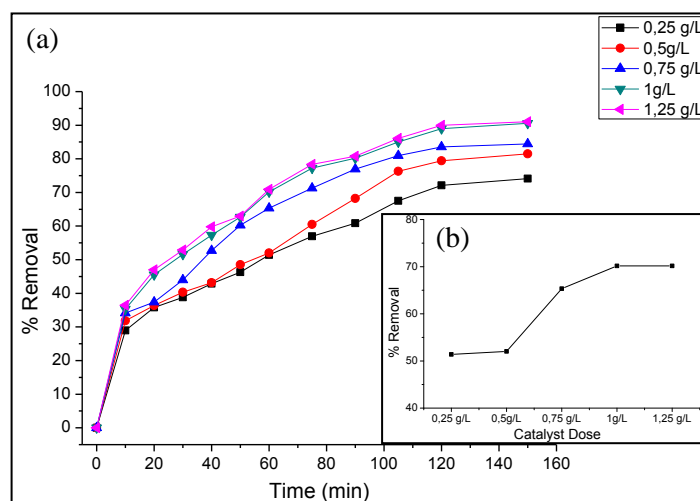


**Figure 6:** Effect of catalyst dose on CV removal in terms of: (a): time - (b): catalyst dose;  $t=75$  min.  
Exp. Conds: (Fe load = 3%,  $[CV]_0 = 20$  ppm,  $[H_2O_2] = 0.39$  M).

There was two critical doses 1g/L and 1,25g/L, at which the removal efficiency was the best, approximately 76%, but with smaller doses 0.25 g/L and 0.5g/L, the removal rate is about 21% in 90min of reaction time (Fig. 6a). The effect of catalyst dose on the discoloration can be explained as follows; when a very small amount of catalyst was used, the catalyst was well dispersed in the reaction medium. Thus, all active surface sites were available. Accordingly, the rate increased with catalyst dose. Once the catalyst dose reached a certain amount (1g/L in this study) the adsorption of CV molecules onto the catalyst surface reached an optimum state. The maintain of stable catalytic activity at higher catalyst doses was because all dye molecules were adsorbed on the catalyst and the addition of a larger amount (1.25 g/L in this study) would have no effect on the degradation rate as it is clearly noticed in Fig. 6b.

▪ *Effect of precursor load*

There is a significant minor activity with the absence of iron oxide in catalytic process, as confirmed previously in the study on comparative of various processes, precisely in the FA/  $H_2O_2$  process. Thereby, the effect of precursor load (0, 1, 3 and 5% Fe-FAC) on the oxidation of CV has been tested (Fig. 7).

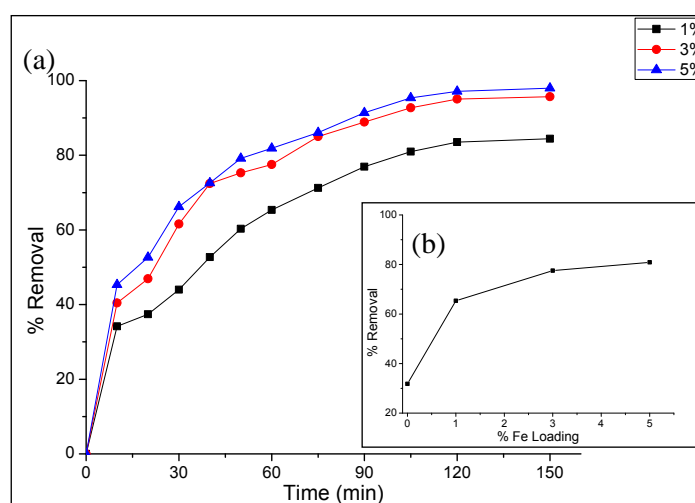


**Figure 7:** Effect of Precursor load on CV removal in terms of: (a): time - (b): % Fe load;  $t=75$ min.  
Exp. Conds: (Catalyst dose = 1g/L,  $[CV]_0 = 20$  ppm,  $[H_2O_2] = 0.39$  M, pH solution, room  $T^\circ$ ).

According to our results, the oxidation efficiency was affected in absence of iron load; it was 31% within 90min compared to 65% for 1% Fe-FAC with an increase of 34% of CV degradation (Fig.6a). When the metal load was varied for the Fe-FAC to 3% the catalytic efficiency improved by only 12% (to 77 %). Thus, no significant change was observed even when the metal load was increased to 5% of catalyst (Fig. 6b). This is the reason why we have chosen the 3% Fe-FAC as the optimum load in the following experiments.

▪ *Effect of initial dye concentration*

Another investigation was done on initial dye concentration to evaluate CV degradation as shown in Fig. 8.

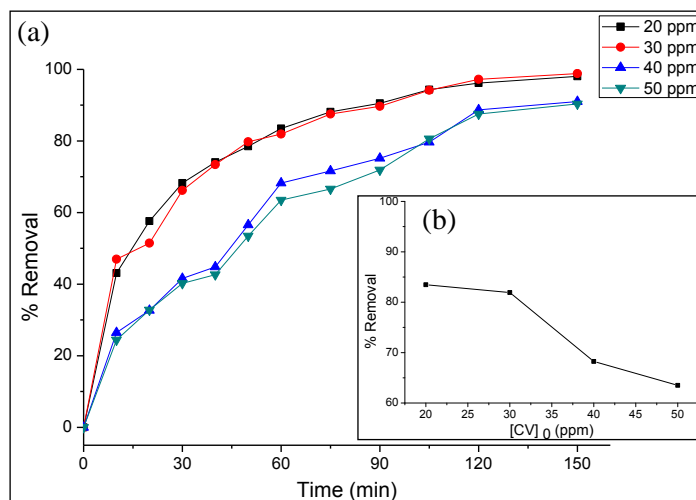


**Figure 8:** Effect of initial dye concentration on CV removal in terms of: (a): time - (b):  $[CV]_0$ ;  $t=75$ min.  
Exp. Conds.: (Catalyst dose = 1g/L, Fe load = 3%,  $[H_2O_2] = 0.39$  M, pH solution, room  $T^\circ$ ).

With the lowest initial dye concentration (20 ppm) the catalytic efficiency presented is about 82%, with only 2% higher than that reached for 30 ppm of initial CV concentration (Fig. 8a). Beyond this concentration the removal rate declined from 80% to 67% for 40 ppm of  $[CV]_0$  and to 62% if  $[CV]_0$  equal 50 ppm (Fig. 8b). The activity lost could have been due to an excessive existence, into dye solution, of CV molecules competing for the active sites among themselves. In that case, it could be concluded that the optimum initial dye concentration is 30 ppm.

• *Effect of oxidant amount*

The influence of oxidant concentration on the degradation of CV was tested by adding different concentrations of hydrogen peroxide (0.19, 0.26, 0.39, 0.78 and 1.96 M) as given in Fig. 9.

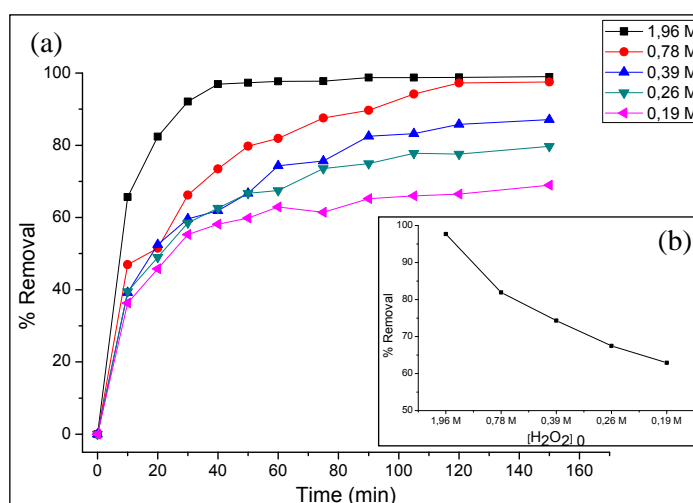


**Figure 9:** Effect of oxidant amount on CV removal in terms of (a): time - (b):  $[H_2O_2]_0$ ;  $t=75$ min.  
Exp. Conds: (Catalyst dose = 1g/L, Fe loading = 3%,  $[CV]_0 = 30$  ppm, pH solution, room  $T^\circ$ ).



The test results in Fig. 9a show that the removal rate when 0.26 and 0.39 M of H<sub>2</sub>O<sub>2</sub> were added into the solution is 68% and 72%, respectively. Moreover, an improved removal rate (82%) was achieved with an increasing of oxidant concentration to 0.78M. This was suggested to be due to deposition of the intermediates on the catalyst surface reducing the efficiency for the oxidation process. Nevertheless, the solution of CV in the higher oxidant concentrations (0.78 and 1.96 M) was decolorized fully, while that in the low 0.19M of H<sub>2</sub>O<sub>2</sub> only 64.5% of CV degradation was attained (Fig. 9b).

- *Effect of pH value*

Industrial wastes usually have various pH values and dye oxidation is strongly affected by varying pH [29].

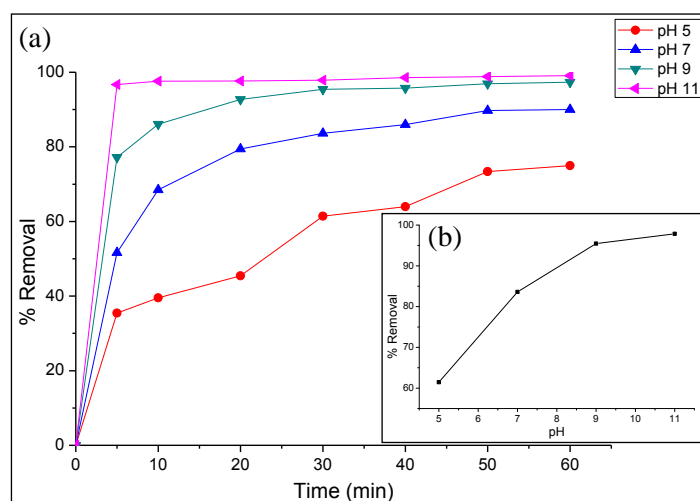


**Figure 10:** Effect of pH value on CV removal in terms of: (a): time - (b): pH solution; t=30min. Exp. Conds.: (Catalyst dose = 1g/L, Fe load = 3%, [CV]<sub>0</sub> = 30 ppm, [H<sub>2</sub>O<sub>2</sub>] = 0.78 M, room T°).

Furthermore, due to the dissolution of the solid catalyst in acidic water to produce ferrous ions in heterogeneous system, the catalyst will inevitably increase the catalytic efficiency of CV when the pH was adjusted below pH 3 [30]. In this study, because the homogeneous catalysis is insignificant at pH > 5 all the degradation processes were studied in the range of pH (5 to 11) and the results are presented in Fig. 10. The pH was adjusted at 5, 7, 9 and 11 using sodium hydroxide (0.1 M) and experiments were run for 60 min.

According to the results presented in the Fig. 10, it is by enhancing the pH values; the catalytic efficiency of the Fe-FAC was sharply accelerated in the first five minutes. Presumably, the catalytic oxidation of CV at the pH solution equal 5.2 was 62% after 30min. When the pH of the feed was increased to neutral value 7, the removal increased by 23% reaching 85%. In addition, the catalytic oxidation was high under alkaline conditions (pH 9 and pH 11) and the degradation rate was 97% and 99%, respectively. The charge on the catalyst surface thus plays an important role for the oxidation reaction as seen from the influence of pH on removal efficiency and reaction time.

- *Effect of solution temperature*

Temperature is one of the most significant factors in the catalytic reactions, especially in the catalytic processes utilized in environmental applications [31]. Therefore, the impact of temperature on the performance of the Fe-FAC was probed and the results are shown in Fig. 11. The oxidative degradation process was performed in the T° range (20 to 50 °C), increased in three steps of 10 °C each. In order to maintain constant operating T°, the reactions were run out under continues stirring and controlled heat using a thermometer.

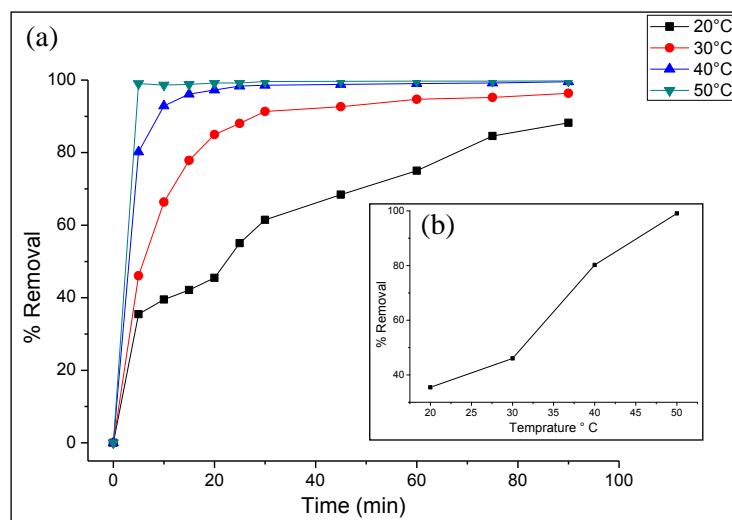


**Figure 11:** Effect of solution temperature on CV removal in terms of: (a): time - (b):  $T^\circ$ ;  $t=5\text{min}$ .  
Exp. Conds. : (Catalyst dose = 1g/L, Fe load = 3%,  $[CV]_0 = 30\text{ ppm}$ ,  $[H_2O_2] = 0.78\text{ M}$ , pH solution).

In Fig. 11a it appeared that, when the temperature increased from 20 to 30°C the degradation of CV was remarkable (from 42% to 78%) in 15 min. While at 40 °C, the rate of oxidative degradation reached to 96 %, this rate could be achieved even near ambient  $T^\circ$  (30°C) after 30 min. The relatively smaller increase of 2% (from 96% to 98%) even when  $T^\circ$  was increased 10°C above 40°C might be due to self decomposition of hydrogen peroxide with rise in temperature and thus, contributing less to CV oxidation. Therefore, 30 °C has been chosen as the optimum  $T^\circ$  value for CV catalytic oxidation.

## Conclusion

In summary, this study investigated the characterization of washed FA and Fe-FAC samples by virtue of XRD and SEM instruments. The FA samples consisted two major mineral phases: firstly, aluminosilicates named Mullite and secondly, silicon oxide that is Quartz with small amount of a non-silicate mineral Calcite. Additionally, the catalyst synthesis process produced more complex aluminosilicates, where the metal Fe was incorporated into the newly formed aluminosilicates. Hence, a third phase appeared, particularly Hematite. Moreover, the results showed that, the particles in washed FA tended to be aggregated into larger particles during washing process. Besides, the iron oxide was distinctly detected and the particle size was clearly decreased.

As well, the wet oxidation of crystal violet with hydrogen peroxide over the iron oxide supported catalysts, displayed excellent removal efficiency. Otherwise, catalytic reaction obeyed pseudo first-order kinetic and almost 100% discoloration of 30 ppm (initial CV concentration) could be obtained after 30 min and less, especially if the initial pH of dye aqueous solution was as high as 9 and above; so the catalyst was enabled at around the neutral and alkaline solution. Undoubtedly, using 1g/L of 3% Fe-FAC with 0.78 M of  $H_2O_2$  was sufficient to bring out that maximum oxidation of the considered pollutant. Indeed, as the solution  $T^\circ$  was increased the catalytic activity improved so the time reaction was reduced.

## References

1. Idrissi M., Miyah Y., Benjelloun Y., Chaouch M., *Journal of Materials and Environmental Science* 7 (2016) 50-58.
2. Santhy K., Selvapathy P., *Bioresource Technology* 97 (2006) 1329-1336.
3. Zhu M. Y., Diao G.W., *Journal of Physical Chemistry C* 115 (2011) 18923-18934.
4. Zhou L., Gao C., Xu W. J., *ACS Applied Materials & Interfaces* 2 (2010) 1483-1491.
5. Liu F., Chung S., Oh G., Seo T.S., *ACS Applied Materials & Interfaces* 4 (2011) 922-927.

6. Boumchita S., Lahrichi A., Benjelloun Y., Lairini S., Nenov V., Zerrouq F., *Journal of Materials and Environmental Science* 7 (2016) 73-84.
7. Bayramoglu G., Altintas B., Arica M., *Chemical Engineering Journal* 152 (2009) 339-346.
8. Visa M., Chelaru A.M., *Applied Surface Science* 303 (2014) 14-22.
9. Lafaye G., Barbier Jr J., Duprez D., *Catalysis Today* 253 (2015) 89-98.
10. Martins R.C., Quinta-Ferreira R.M., *Industrial & Engineering Chemistry Research* 48 (2009) 1196-1202.
11. Bharati D., Bhattacharyya K.G., *Journal of Environmental Management* 150 (2015) 479-488.
12. Munoz M., Domínguez P., De Pedro Z.M., Casas J.A., Rodriguez J.J., *Applied Catalysis B: Environmental* 203 (2017) 166-173.
13. Suchithra P.S., Vazhayal L., Mohamed A.P., Ananthakumar S., *Chemical Engineering Journal*. 200(2012) 589-600.
14. Kim H.J., Pant H.R., Choi N.J., Kim C.S., *Chemical Engineering Journal* 230 (2013) 244-250.
15. Zhang J., Wang B., Cui H., Li C., Zhai J., Li Q., *Journal of Rare Earths* 32(2014) 1120-1125.
16. Hu Y, Zhang P., Li J., Chen D., *Journal of Hazardous Materials* 299 (2015) 149-157.
17. Koshy N., Singh D.N., *Journal of Environmental Chemical Engineering* 4 (2016) 1460-1472.
18. Fan H. J., Lu C.S., Lee W. L. W., Chiou M. R., Chen C.C., *Journal of Hazardous Materials* 185 (2011) 227-235.
19. Bellarbi A., Monkade M., Zradba A., Laameyem A., *Journal of Environmental Science & Engineering A* 4 (2015) 286-294.
20. Liu L., Zheng L., Li X., Xie S., *Journal of Hazardous Materials* 162 (2009) 161-173.
21. Chen C.C., Chen W.C., Chiou M.R., Chen S.W., Chen Y.Y, Fan H J. *Journal of Hazardous Materials* 196 (2011) 420-425.
22. Benjelloun Y., Miyah Y., Idrissi., Boumchita S., El Ouali Lalami A., Zerrouq F., *Journal of Materials and Environmental Science* 7 (2016) 9-17.
23. Kutchko B.G., Kim A.G., *Fuel* 85 (2006) 2537-2544.
24. Miyah Y., Lahrichi A., Idrissi M., Boujraf S., Taouda H., Zerrouq F., *Journal of the Association of Arab Universities for Basic and Applied Sciences*, (2015). <http://dx.doi.org/10.1016/j.jaubas.2016.06.001>.
25. Kim H. J., Joshi M.K., Pant H.R., Kim J. H., Lee E., Kim CS., *Colloids and Surfaces A: Physicochemical and Engineering Aspects* 469 (2015) 256-262.
26. Guiza S., Bagane M., *Journal of Water Science* 26 (2013) 39-50.
27. Xie J., Kayali O., *Construction and Building Materials* 122 (2016) 36-42.
28. Zhu M., Meng D., Wang C., Di J., Diao G., *Chinese Journal of Catalysis* 34 (2013) 2125-2129.
29. Lu W., Chen W., Li N., Xu M., Yao Y., *Applied Catalysis B: Environmental* 87 (2009) 146-151.
30. Liou M.J., Lu M. C., *Journal of Hazardous Material* 151 (2008) 540-546.
31. Rayati S., Sheybanifard Z., *Comptes Rendus Chimie* 19 (2016) 371-380.

(2017) ; <http://www.jmaterenvironsci.com>